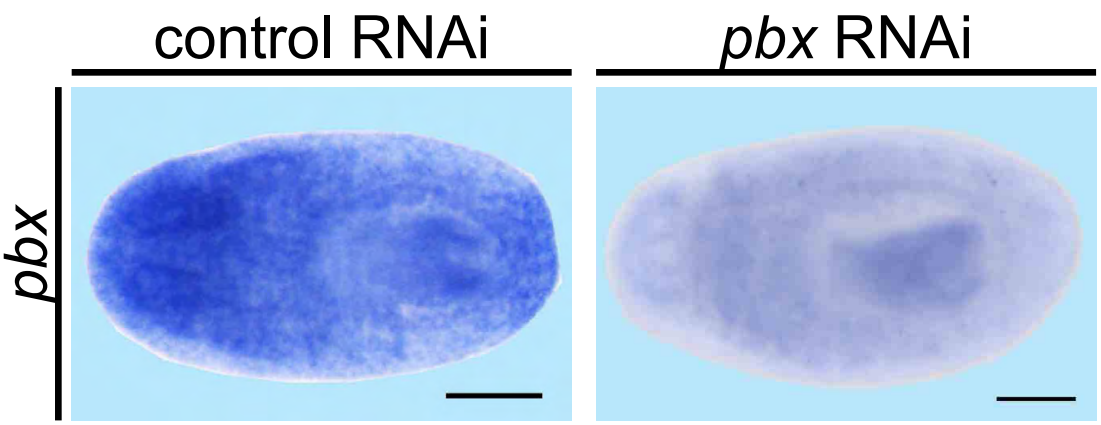

Fig. S1. RNAi of *pbx* by feeding results in reduction of *pbx* mRNA. Worms were fed with control or *pbx* RNAi food as described in Materials and methods. Two days after the last feeding worms were transversely amputated. Day 6 regenerating worms were fixed for whole-mount ISH. Control RNAi animals (6/6) exhibited broad *pbx* expression whereas *pbx(RNAi)* animals (6/6) had only light background staining.

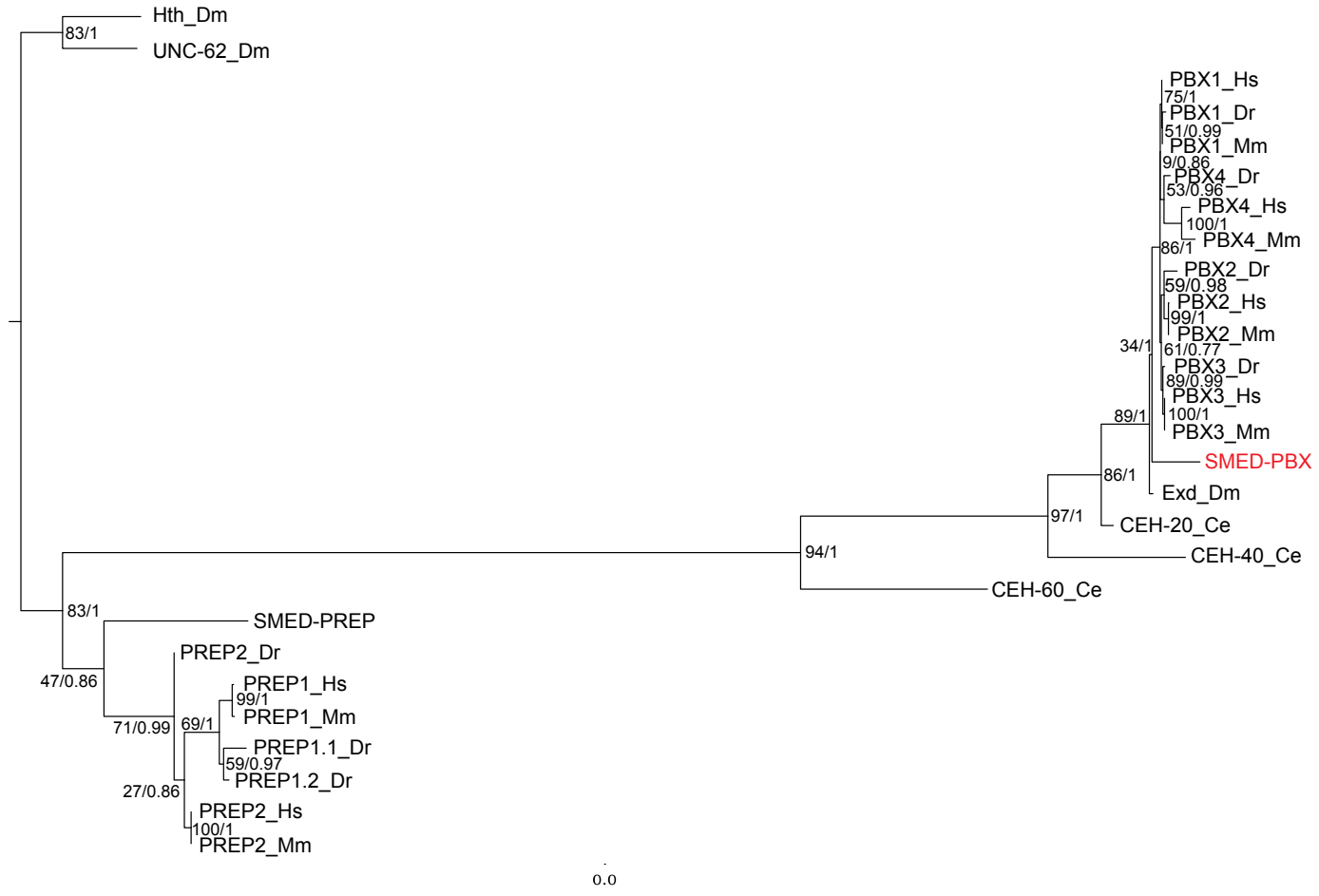

Fig. S2. Phylogenetic analysis of SMED-PBX. Seventeen Pbx, eight Prep and two Meis proteins from diverse organisms were aligned using ClustalW with default settings and trimmed with Gblocks. Maximum likelihood analyses were run using PhyML with 100 bootstrap replicates, the WAG model of amino acid substitution, four substitution rate categories and the proportion of invariable sites estimated from the dataset. The result provides strong support for SMED-PBX (highlighted in red) to be a member of the PBX subfamily of the TALE protein family. All ML bootstrap values are shown. Hs, *Homo sapiens*; Mm, *Mus musculus*; Dr, *Danio rerio*; Dm, *Drosophila melanogaster*; Ce, *Caenorhabditis elegans*; Smed, *Schmidtea mediterranea*.

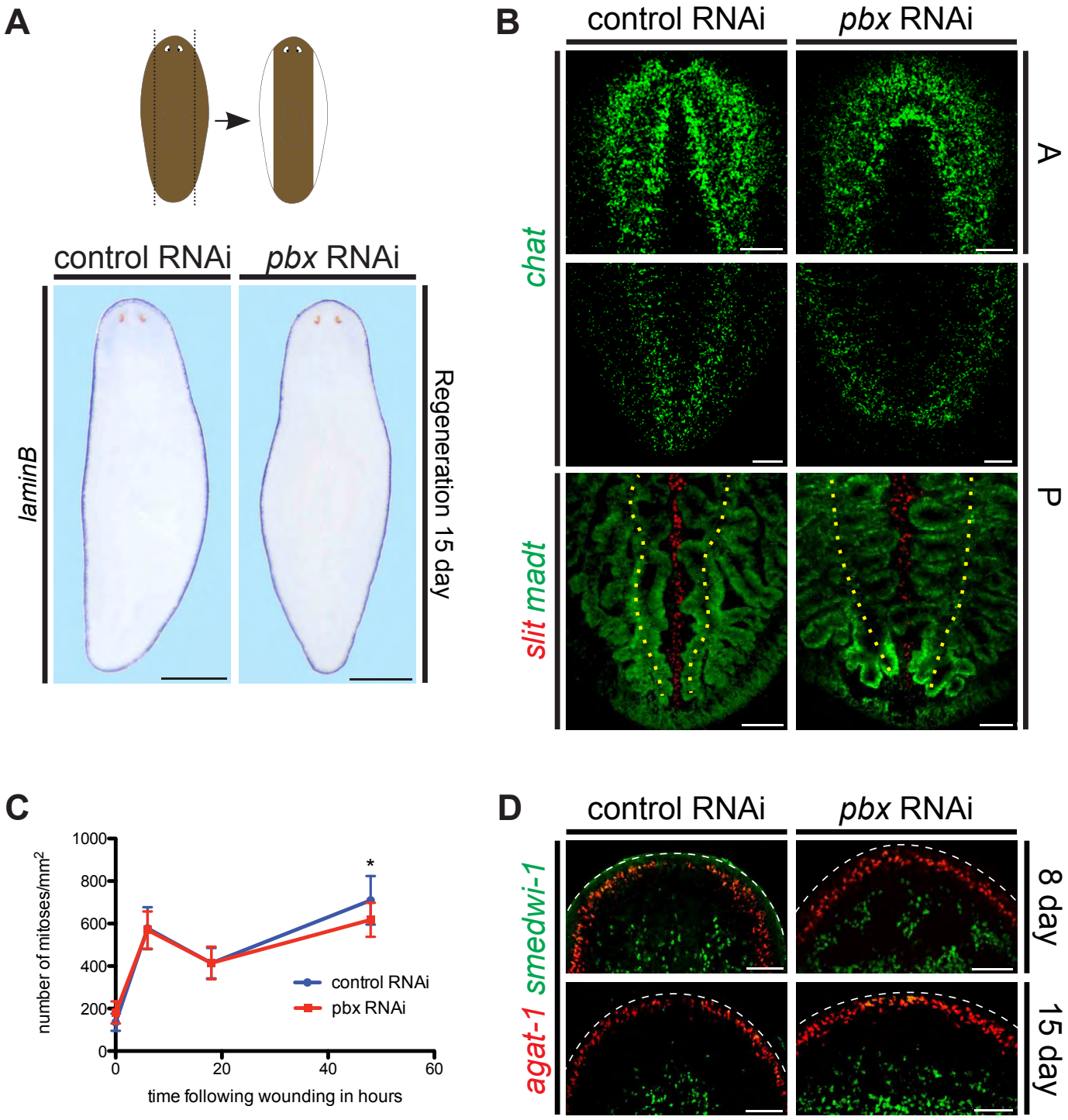

Fig. S3. Additional analysis of the *pbx(RNAi)* phenotype, including neoblasts and late regeneration time points. (**A**) *pbx(RNAi)* animals exhibited normal lateral boundary regeneration 15 days post-amputation (control, *n*=13/14; *pbx* RNAi, *n*=19/21 have uninterrupted *laminB* domains). Cartoon depicts lateral amputation. Scale bars: 0.5 mm. (**B**) *pbx(RNAi)* animals exhibited fused cephalic ganglion lobes (control, *n*=0/6; *pbx* RNAi, *n*=6/6) and truncated posterior nerve cords (control, *n*=0/6; *pbx* RNAi, *n*=6/6) that appeared joined at the posterior end (control, *n*=0/5; *pbx* RNAi, *n*=3/6) at 15 days post-amputation. *pbx(RNAi)* animals displayed widened *slit* expression domains (control, *n*=0/6; *pbx* RNAi, *n*=4/5) and longer medial intestinal branches adjacent to the ventral *slit* expression domain (control, *n*=0/6; *pbx* RNAi, *n*=2/5) at 15 days post-amputation. Yellow dotted lines indicate primary posterior intestinal branches. Scale bars: 200 μm for *chat*; 100 μm for *slit+MADT*. (**C**) Assay of wound response by mitoses per unit area shows no significant difference in mitotic cell density between control and *pbx(RNAi)* animals at the 6 hour global response peak and lower mitotic density in *pbx(RNAi)* animals at the 48 hour missing tissue response peak (**P*<0.05, *t*-test). Error bars represent s.d. (**D**) *pbx(RNAi)* animals exhibited reduced separation between *smedwi-1*$^{+}$ and *agat-1*$^{+}$ domains at 8 days post-amputation (control, *n*=1/6; *pbx* RNAi, *n*=6/6) and 15 days post-amputation (control, *n*=0/6; *pbx* RNAi, *n*=5/5). White dashed lines indicate head rim. Scale bars: 100 μm.

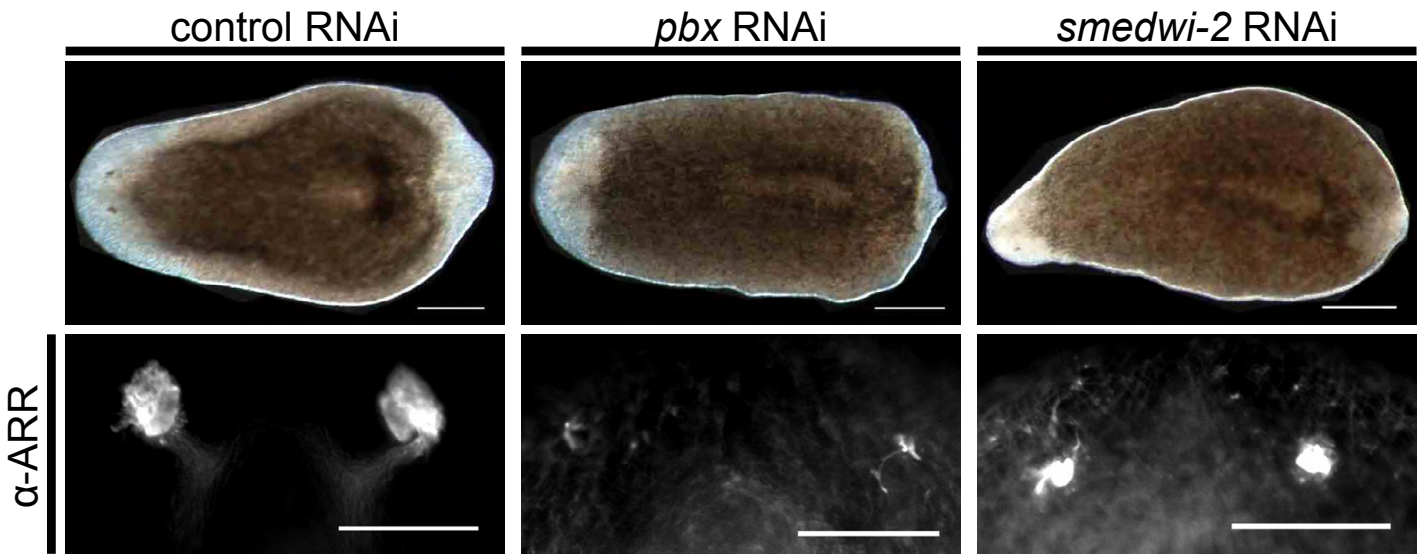

Fig. S4. The influence of blastema size on eye regeneration. Worms were injected with dsRNA against control, *pbx* or *smedwi-2* at 600 μg/ml to achieve weak RNAi. Both control (*n*=10) and *pbx(RNAi)* (*n*=10) animals regenerated blastemas with similar size but *smedwi-2(RNAi)* (*n*=8) animals produced smaller blastemas. However, *pbx(RNAi)* animals exhibited less eye regeneration than did *smedwi-2(RNAi)* animals, as shown with anti-ARRESTIN labeling of photoreceptor neurons. Scale bars: 100 μm.

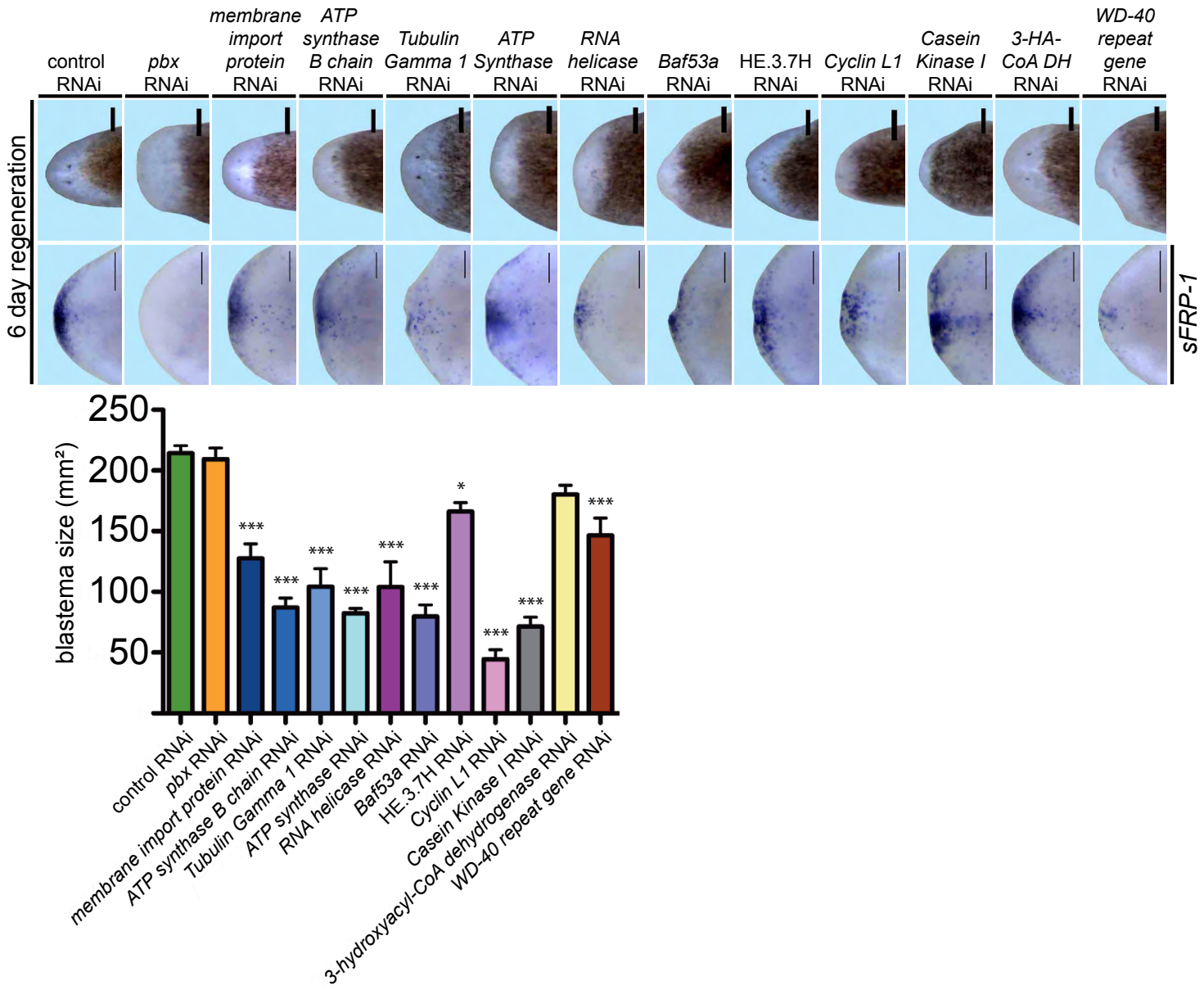

Fig. S5. Examination of *sFRP-1* expression in head blastemas following RNAi of 11 randomly selected genes that affect blastema formation. RNAi of 11 genes reported to be required for blastema formation by Reddien et al. (Reddien et al., 2005a) resulted in animals with head blastemas smaller than those of *pbx(RNAi)* animals, but more *sFRP-1* expression in each case. Animals were fed RNAi food three times, transversely amputated and fixed 6 days after amputation for *in situ* hybridization. Quantification of blastema size is shown in the bottom panel (one-way ANOVA test followed by a Dunnet post-hoc test; ***$P \leq 0.001$ between the experimental condition and the control; *$P \leq 0.05$ between the experimental condition and the control. cDNA clones used for each gene are as follow: *membrane import protein* (HE.4.1B), *ATP synthase B chain* (HE.4.2D), *Tubulin Gamma 1* (NBE.8.2D), *ATP Synthase* (NBE.8.9G), *RNA helicase* (HE.2.9G), *Baf53a* (HE.3.10F), *cyclin L1* (NBE.2.9B), *casein kinase I* (HE.3.9F), *3-hydroxyacyl-CoA dehydrogenase* (NBE.2.3C) and *WD-40 repeat* (NBE.2.9G).

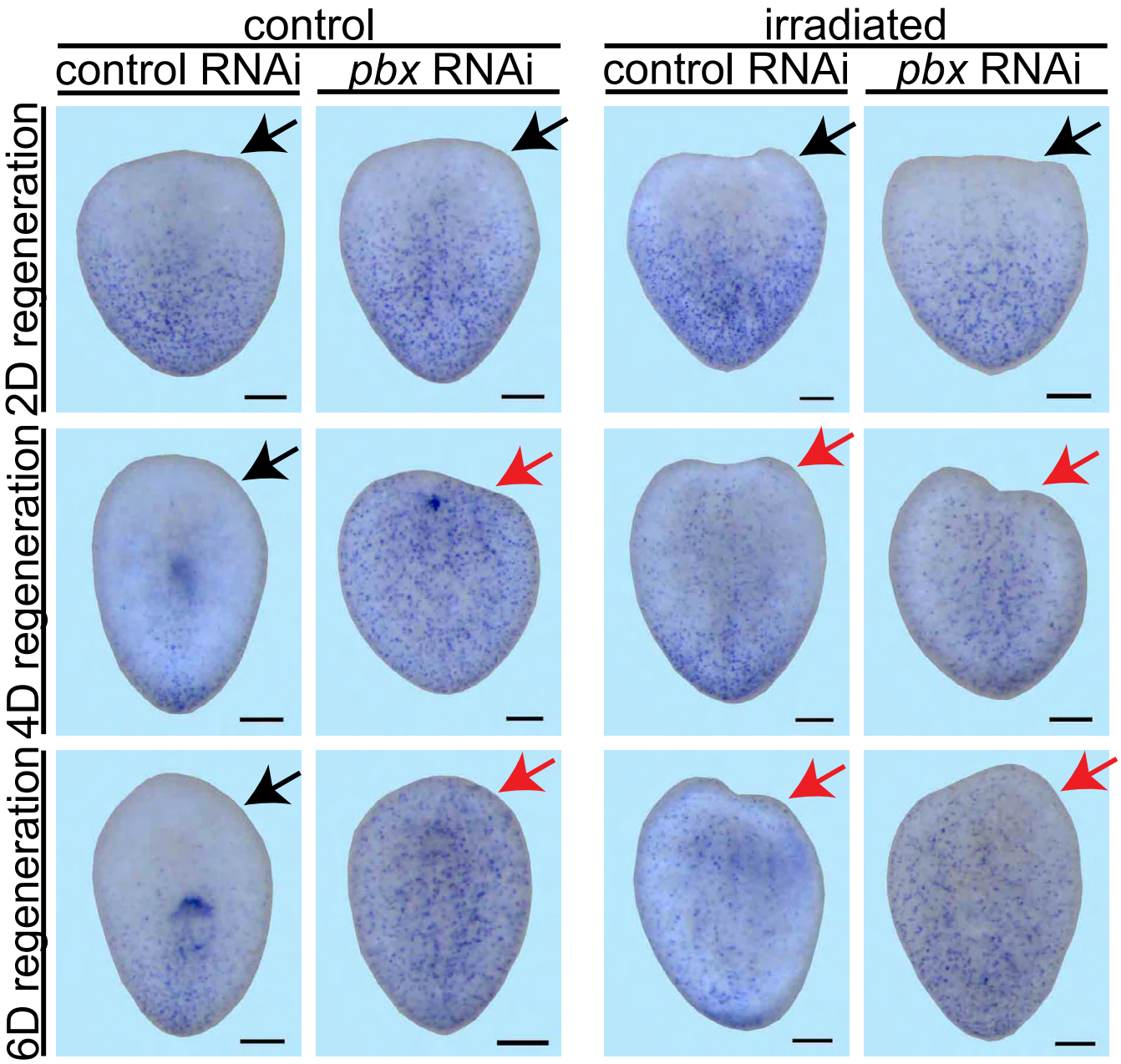

Fig. S6. *pbx* is required for irradiation-sensitive rescaling of the *wntP-2/wnt11-5* expression domain in regenerating tail pieces. Animals were fed with RNAi food four times, transversely amputated and fixed at the indicated regeneration time points for *in situ* hybridization with a *wntP-2* RNA probe. Irradiated animals were exposed to 6000 rads of radiation 4 days prior to amputation. Control animals exhibited retraction of the *wntP-2* expression domain to the tail tip at 4 days following amputation [as described by Peterson et al. (Petersen et al., 2009b)]. *wntP-2* expression subsequently expanded anteriorly to approximately where the new pharynx was forming at 6 days following amputation. Irradiated animals and *pbx(RNAi)* animals displayed initial clearing of *wntP-2* expression from the wound site (2 days after amputation) followed by expansion back towards the wound (4 days after amputation) ($n \geq 7$ for each condition). This behavior of *wntP-2* expression in irradiated tail fragments is as described by Gurley et al. (Gurley et al., 2011). Black arrows, normal expression pattern; red arrows, aberrant expression pattern. Scale bars: 100 μm.

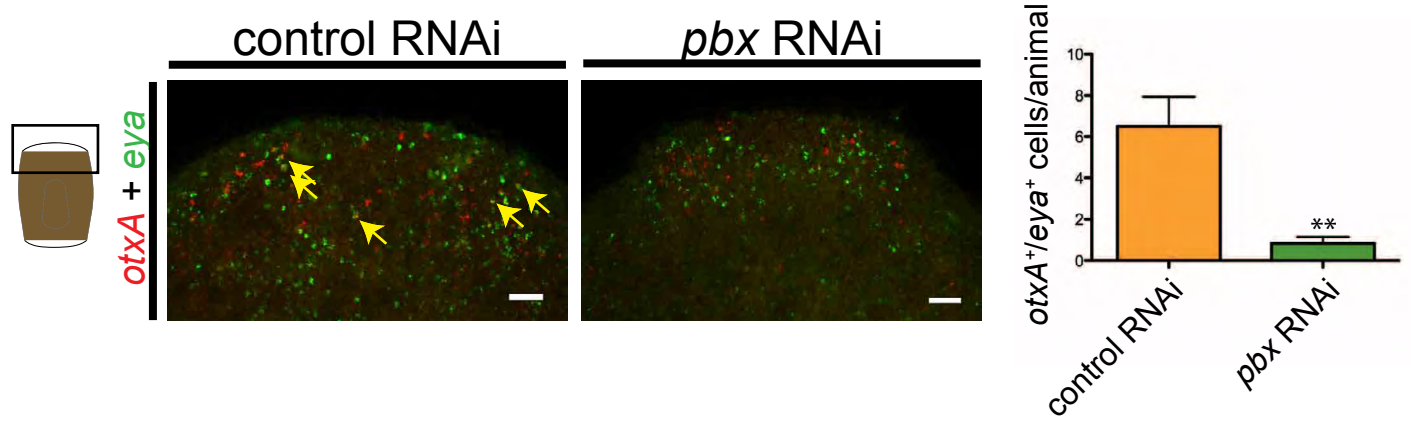

Fig. S7. Eye progenitor formation in *pbx(RNAi)* animals. *pbx(RNAi)* animals are required for *otxA*$^+$ *eya*$^+$ eye progenitor formation at 48 hours after amputation. Worms were fed with RNAi food four times, transversely amputated and fixed after 48 hours of amputation. FISH was performed to examine presence of *otxA*$^+$ *eya*$^+$ double-positive cells in or near the head blastema. Quantification of the number of double-positive cells is shown at right (n=6 for both conditions, **P=0.0031, t-test). Error bars represent s.e.m.

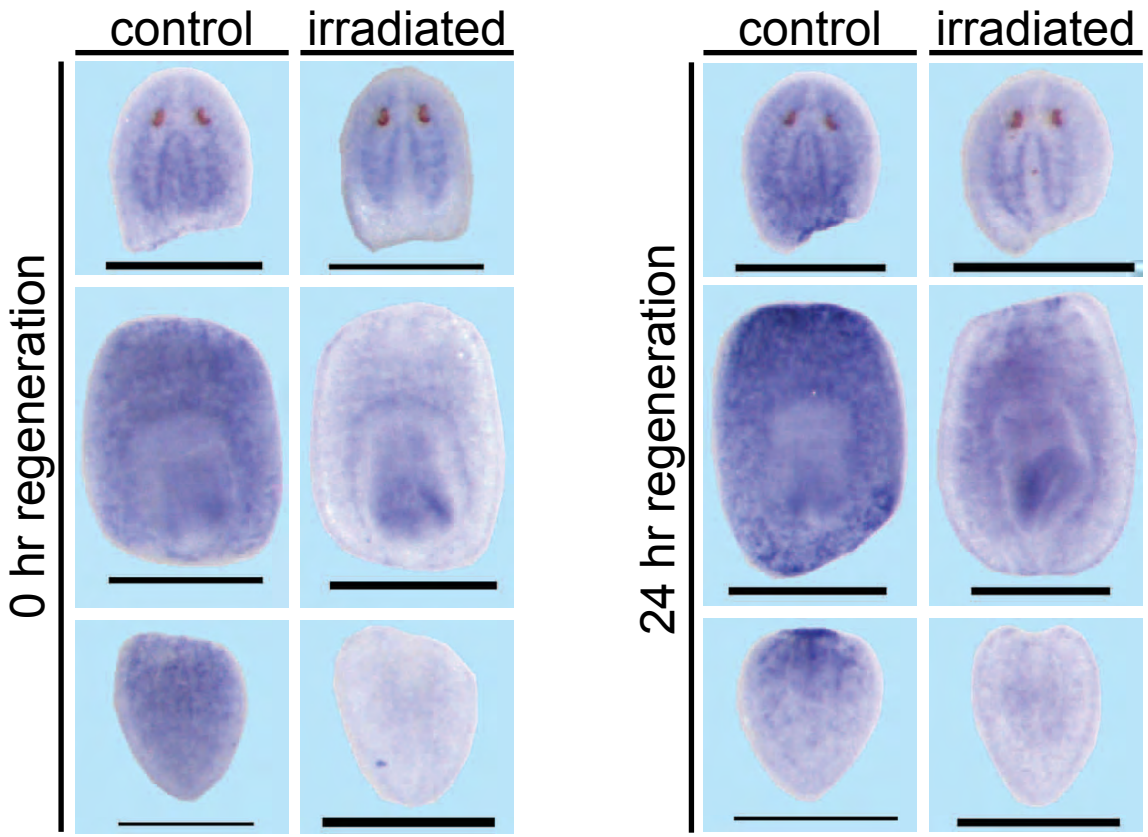

Fig. S8. *pbx* expression during early regeneration time points. Worms were transversely amputated and *pbx* expression accumulated at wound sites at 24 hours (n=6) after cutting and compared with freshly amputated animals (n=6). Worms were irradiated 4 days before amputation. Scale bars: 200 μm.

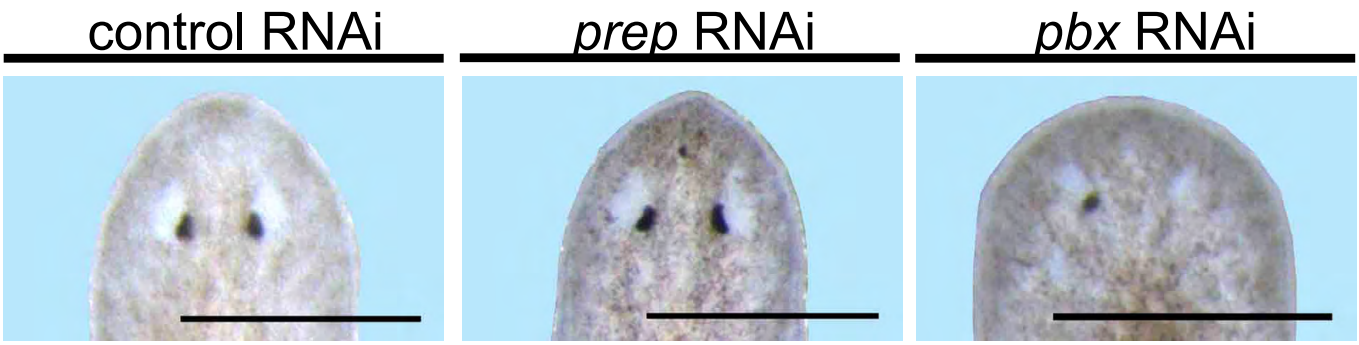

Fig. S9. *pbx(RNAi)* causes eye maintenance defects in unamputated animals. Light microscope images of the eyes of unamputated animals following 6 weeks of RNAi. Scale bars: 200 μm.

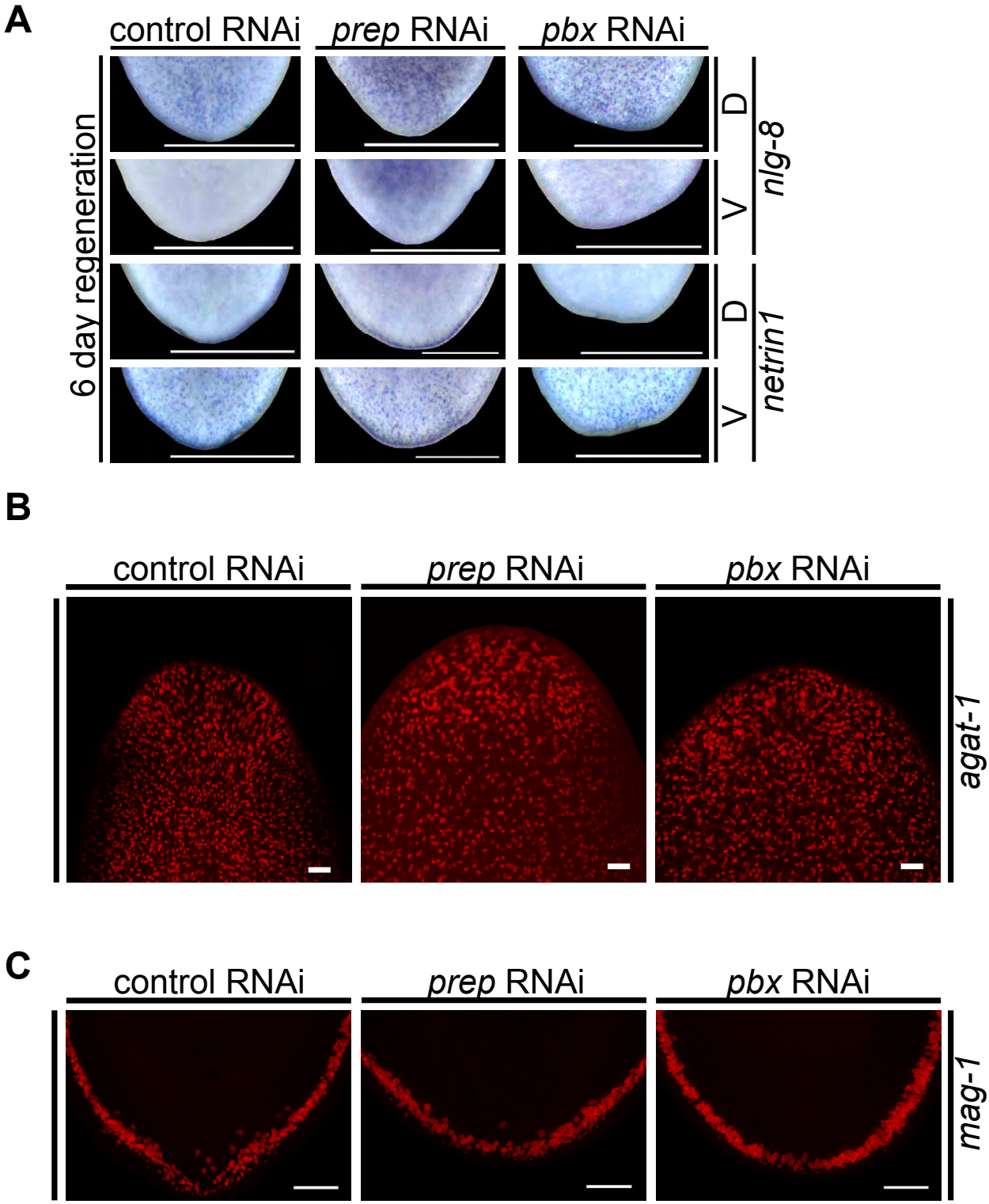

Fig. S10. Additional analysis of the *pbx(RNAi)* phenotype regenerating animals after long-term RNAi: expression of *nlg-8* and *netrin1* and neoblast differentiation. Animals underwent 6 weeks of RNAi, followed by amputation, and were analyzed 6 days after amputation. (**A**) Differential gene expression along the DV axis remained normal as shown by dorsal expression of *nlg-8* in regenerating posterior blastemas (control, *n*=16/16; *prep* RNAi, *n*=16/16; *pbx* RNAi, *n*=15/15) and ventral expression of *netrin1* (control, *n*=15/15; *prep* RNAi, *n*=16/16; *pbx* RNAi, *n*=15/15). (**B**) *agat-1*$^{+}$ neoblast progeny were also normal (control RNAi, *n*=15/15; *prep* RNAi, *n*=16/16, *pbx* RNAi; *n*=14/14 regenerating fragments). (**C**) *mag-1*$^{+}$ cells were regenerated (control RNAi, *n*=15/15; *prep* RNAi, *n*=16/16; *pbx* RNAi, *n*=14/14 regenerating fragments). Scale bars: in A, 500 μm; in B,C, 100 μm.

Table S1. List of primers used in this study. T7 promoter sequences and AttB1/2 adaptor sequences are shown in orange and red, respectively.

For riboprobes		
Smed-sFRP-1	TTGAATTCATGGAAATGACCAA	forward
Smed-sFRP-1	CATGTAATACGACTCACTATAGGGAATCAATGAAATGTTTTGTTGTGA	reverse
Smed-ndl-4	TGCAAATTGGTTCCACGTTA	forward
Smed-ndl-4	CATGTAATACGACTCACTATAGGGGAAGGCGACGACGAATTTT	reverse
Smed-prep	GCAACAAGCTGATCCTGGTT	forward
Smed-prep	CATGTAATACGACTCACTATAGGGGGAATGGTTGAAAACCGAAT	reverse
Smed-wnt2	ATCTTTCTTCACCTGGTTCTGG	forward
Smed-wnt2	CATGTAATACGACTCACTATAGGGTGATGAAGCGAGAGAAAATGAA	reverse
Smed-ndl-3	TGGAAATAATCTGTCCGCTTG	forward
Smed-ndl-3	CATGTAATACGACTCACTATAGGGGGATGAAGGATAATACGGATGG	reverse
Smed-wntP-2	TTAAATGTTCTAAGCCAAAACAACA	forward
Smed-wntP-2	CATGTAATACGACTCACTATAGGGAAAACTTTTATGATCAATCTGAATGC	reverse
Smed-abd-Ba	TTTTAAAGCATTGGATTTTCAC	forward
Smed-abd-Ba	CATGTAATACGACTCACTATAGGGAAGCTTGTTGATTAGGATTTCT	reverse
Smed-wnt11-1	GGCCGTTGTTCATGCTTTTA	forward
Smed-wnt11-1	CATGTAATACGACTCACTATAGGGCATGAGCCAGTAAATGAAATGGT	reverse
Smed-fz-4	CATGTAATACGACTCACTATAGGGGGAATAGCCCAACTCACCAA	reverse
Smed-fz-4	TGCCGAATTTAGTTGGAAGC	forward
Smed-wnt1	CCTCAAAATCGAATTTTACACTCA	forward
Smed-wnt1	CATGTAATACGACTCACTATAGGGTGGGACAAAAATAAAATTCCACA	reverse
Smed-notum	AAAATTTCTGAGGATCGAAAAA	forward
Smed-notum	CATGTAATACGACTCACTATAGGGTGAAGCTAGATTTATGTGAAAAACCA	reverse
Smed-pbx	CACCAGCCTCCGAGTAGTTG	forward
Smed-pbx	CATGTAATACGACTCACTATAGGGTGTCAATGCTATCAAGGAATCAA	reverse
cubilin	Scimone et al., 2011	
chat	Wagner et al., 2011	
mag-1	H1.3B	
laminB	Reddien et al., 2007	
otxA	Lapan and Reddien, 2011	
eya	Lapan and Reddien, 2011	
Smed-bmp4	Reddien et al., 2007	
Smed-admp	Gaviño and Reddien, 2011	

For RNAi		
Smed-pbx	CATGTAATACGACTCACTATAGGGCACCAGCCTCCGAGTAGTTG	forward
Smed-pbx	TGTCAATGCTATCAAGGAATCAA	reverse
Smed-pbx	CACCAGCCTCCGAGTAGTTG	forward
Smed-pbx	CATGTAATACGACTCACTATAGGGTGTCAATGCTATCAAGGAATCAA	reverse
Smed-prep	AAGCTGGAGCTCCACCGCGGtgaacaagcaactgcctcac	forward
Smed-prep	GGGCGAATTGGGTACCGGGcctgttgctcttcccatgat	reverse

Movie 1. Control RNAi animal at homeostasis day 45+ exhibiting normal locomotion.

Movie 2. *pbx(RNAi)* animal at homeostasis day 45+ exhibiting locomotive defect.

Movie 3. ***prep(RNAi)*** **animals at homeostasis day 45+ exhibiting normal locomotion.**